

Mechanical responses of wood to repeated loading

M. Kohara^a, K. Ando^b and T. Okuyama^b

^aStructural Formation Process Department, National Industrial Research Institute of Nagoya,
Hirate-cho 1, Kita-ku, Nagoya 462, Japan

^bSchool of Agricultural Sciences, Nagoya University,
Nagoya 464-01, Japan

In this paper, a partitioning scheme of energy loss (EL) on the basis of its dependency on stress amplitude was proposed. EL was partitioned into two terms. One is due to linear viscoelasticity, and the other should be related to fatigue damage. Prediction of fatigue lifetime in terms of EL was outlined based on this scheme. An empirical formula that describes the dependency of EL on stress amplitude was proposed. The variation of EL behavior with species was described using this formula. A parallelism between EL and acoustic emission (AE) was also pointed out.

1. INTRODUCTION

For more safe and economical utilization of wood and wood-based material as members of construction, furniture, hand tools, sports instruments etc., it is needed to realize its behavior under repeated load condition of rather larger stress ranges. Responses of wood under repeated loading are characterized by its energy loss behavior. Many studies have been done based on the theory of linear viscoelasticity, however, the scope of the theory has not been extended into the larger stress range which consequences finally the fatigue fracture of the material.

In this paper, we proposed a partitioning scheme of energy loss based on its dependence on stress amplitude. By using this scheme, we aimed to realize the behavior of wood in rather larger stress ranges.

2. EXPERIMENTS

Five species—spruce, fir, hinoki, hemlock, and buna were used. The dimensions of the flat sawn part of the small clear tensile specimens were 60, 15, and 3 mm for L-, R-, and T-directions, re-

spectively. The testing chamber was maintained at 20°C, 65% R.H. air condition.

The following three loading methods were employed. *Static test*: The loading speed was set at 1.67 kgf s⁻¹. *Incremental step test*: Applied load amplitudes were incremented stepwisely by 5.0 kgf. Three cycles of load were applied for the measurement of EL, and the procedure was repeated three times for each step with 20–30 s interval (see Fig. 1).

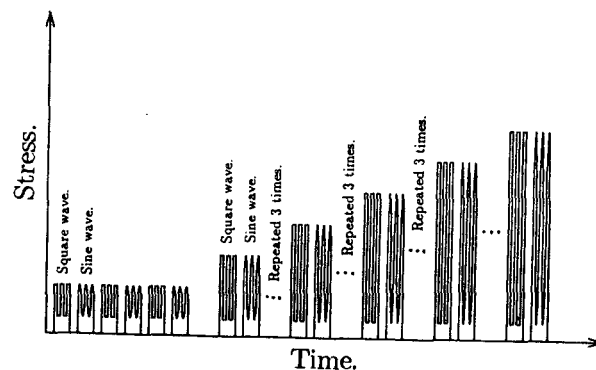


Fig. 1 Schematic diagram of the incremental step test.

Fatigue test: Repeated loads of fixed amplitudes were applied till fracture.

An electro-hyroservo universal testing machine, MTS-812, was used for all experiments. It

included an extensometer with a span of 25 mm, and a load cell of 5 ton capacity. The applied load frequency was 1 Hz, and the applied wave forms were square wave and sine wave.

AE signals were measured and analyzed by using Shimadzu SAE-100A system. Differential type AE transducers of 200 kHz resonance frequency (S20DSA) were used. Band pass filters of 100–500 kHz range were adopted, and the slicer level for AE counting was set at 40 mV.

3. RESULTS AND DISCUSSION

3.1 Limit stress of linear viscoelasticity

A typical result of multiple step tests is shown in Fig. 2, where H_c is energy loss per cycle, and σ is stress amplitude. The values of H_c/σ^2 (vertical axis) were constant below a certain stress amplitude— σ_0 . In this stress range ($\sigma < \sigma_0$), the energy losses are proportional to the squares of stress amplitudes ($H_c \propto \sigma^2$). The energy loss behavior in this stress range is entirely explained by the theory of linear viscoelasticity. We conclude that this threshold σ_0 can be regarded as the limit stress of the linear viscoelasticity. It should also be pointed out that σ_0 is independent of wave forms [2].

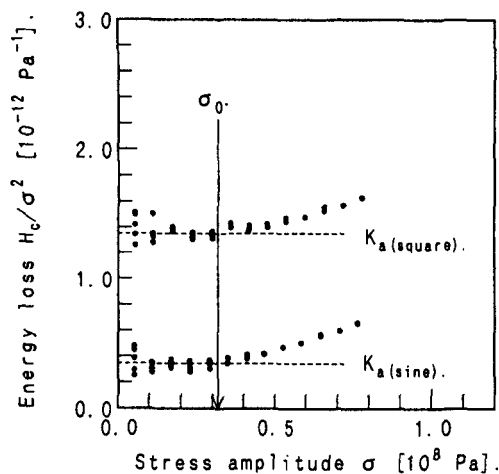


Fig. 2 Relationships between energy losses H_c/σ^2 and stress amplitudes σ . Illustrating determination of K_a and σ_0 .

3.2 Partitioning scheme of energy loss

Energy loss per cycle H_c should be partitioned

into two terms as follows: (see also Fig. 6)

$$H_c = H_a + H_b \quad (1)$$

where, H_a is the term which is entirely explained by linear viscoelasticity, and H_b is the excess part of energy loss (defined by $H_c - H_a$). We consider that the term H_b should be related to the fatigue damage caused by repeated loading.

3.3 Prediction of fatigue lifetime (1)

We proposed a Manson-Coffin type criterion of fatigue lifetime in terms of energy loss H_b as follows:

$$H_b \cdot N_f^\alpha = C \quad (2)$$

where, N_f is the repetition number of load to failure; α and C are constants. (This criterion can be related to the cumulative energy to failure.) Transform this equation into a logarithm, we obtain

$$\log N_f = -(1/\alpha) \log H_b + (1/\alpha) \log C. \quad (3)$$

We fitted this equation into the results of fatigue tests (shown in Fig. 3), and obtained the following values as results of linear regression: $-(1/\alpha) = 1.99$; $\log C = 2.76$ (where correlation coefficient $r = 0.90$). Thus we obtained the values for constants appeared in the criterion, $\alpha = 0.503$, $C = 24.4 \times 10^4 \text{ J m}^{-3}$.

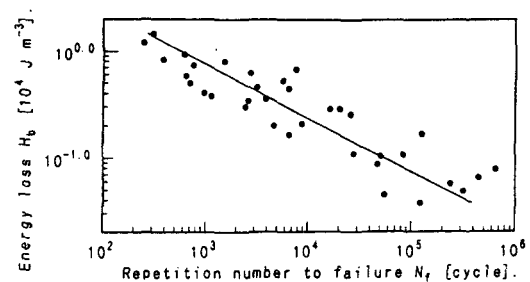


Fig. 3 Relationships between energy losses H_b and fatigue lifetimes N_f .

3.4 Prediction of fatigue lifetime (2)

In a previous section (3.3), we implicitly postulated that the amount of energy loss H_b is constant during the whole fatigue process. In case of fatigue by square wave, this postulation is valid. However, in case of fatigue by sine wave, the postulation is not valid, as shown in Fig. 4. When the square wave was applied, the values of H_c seem almost constant. On the other hand, energy loss decreased in a semi-log scale when the sine wave

was applied. In this case, we need to consider the total of energy loss H_b to failure, $\sum H_b$. Now, we introduce a new criterion of fatigue failure in terms of $\sum H_b$ as follows:

$$\sum H_b \cdot N_f^{\alpha-1} = C \quad (4)$$

Transform Eq. 4 into logarithm, we obtain

$$\log N_f = -\frac{1}{\alpha-1} \log \sum H_b + \frac{1}{\alpha-1} \log C. \quad (5)$$

Fitting this equation to results of fatigue tests, we obtained the following values for the constants of the equation: $\alpha = 0.184$; $C = 2.23 \times 10^4 \text{ J m}^{-3}$.

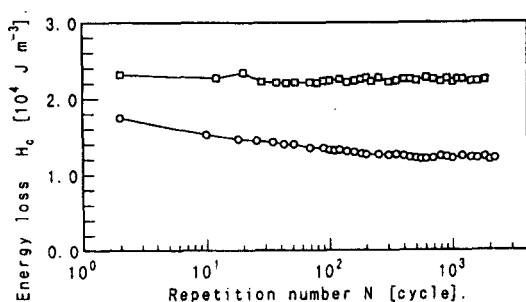


Fig. 4 Variations of energy losses during fatigue tests.

Legend: □: Square wave, ○: Sine wave.

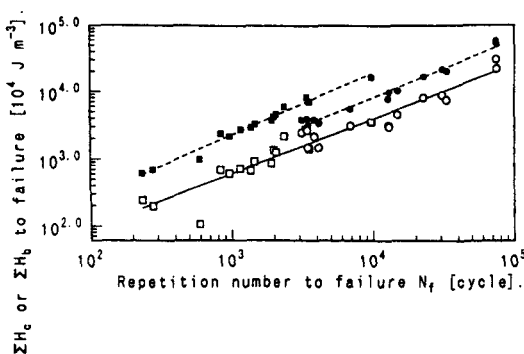


Fig. 5 Relationships between total energy losses $\sum H_c$, $\sum H_b$ to failures and fatigue lifetimes N_f .

Legend: ■: $\sum H_c$ with square wave, ●: $\sum H_c$ with sine wave, □: $\sum H_b$ with square wave, ○: $\sum H_b$ with sine wave.

3.5 Formulation of energy loss

Based on the results of multiple step tests, we formulated the dependency of energy losses H_c on

stress amplitudes σ as follows:

$$H_c(\sigma) = K_a \cdot \sigma^2 + K_b \cdot (\sigma - \sigma_0)^n \quad (6)$$

Fig. 6 illustrates schematically this relationship. Remark that the constant K_a is dependent on wave forms. On the other hand, constants K_b , n , and σ_0 are not affected by wave form.

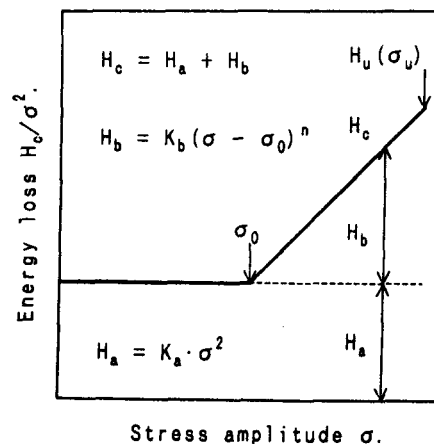


Fig. 6 Schematic diagram of the relationships between energy losses H_c/σ^2 and stress amplitudes σ .

3.6 Relationship between AE and EL

A typical result of incremental step test is shown in Fig. 7. Parallelism can be pointed out between AE behavior and non-linear part of energy loss in rather larger stress ranges.

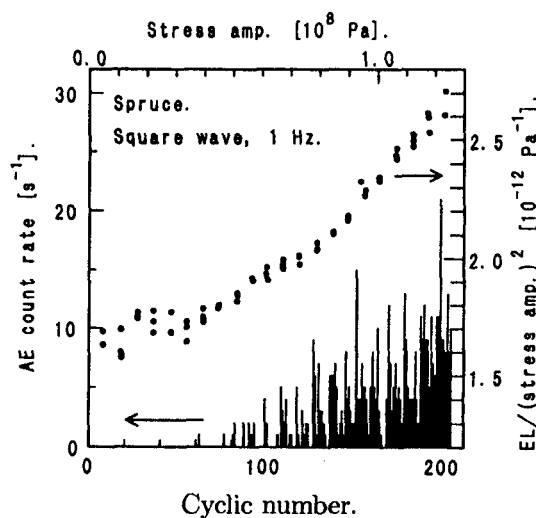


Fig. 7 A typical result of incremental step test.

3.7 Variation of energy loss with species

As shown in Fig. 8, the dependency of energy loss H_c on stress amplitude σ varies remarkably with species. We fitted the formula proposed in a previous section (3.5) and obtained the values of the constants in the formula as shown in Table 1. We also found that K_b and n are independent of K_a [3]. The fact implies that the energy loss behavior in the larger stress range is not predictable from the behavior in the smaller stress range.

4. CONCLUSION

By using the energy loss partitioning scheme, mechanical responses of wood in rather larger stress ranges can be consistently described and formulated. Since our partitioning scheme was derived from macroscopic and phenomenological

viewpoints, more effort is needed to establish the linkage with microscopic and mechanistic approaches.

REFERENCES

1. Mitsuhiro KOHARA and Takashi OKUYAMA: *Mokuzai Gakkaishi*, November 1993, Vol. 39, No. 11, pp. 1226-1230.
2. Mitsuhiro KOHARA and Takashi OKUYAMA: *Mokuzai Gakkaishi*, May 1994, Vol. 40, No. 5, pp. 491-496.
3. Mitsuhiro KOHARA and Takashi OKUYAMA: *Mokuzai Gakkaishi*, August 1994, Vol. 40, No. 8, pp. 801-809.
4. Mitsuhiro KOHARA and Kosei ANDO: Abstracts of the 40th Anniversary Conference of the Japan Wood Research Society, 1995, p. 552.

Table 1. The summarized results of the incremental step tests.

Species	Number of specimens	K_a [10^{-12} Pa $^{-1}$]		K_b [10^{-12}]		n		σ_0 [10^8 Pa]	σ_u [10^8 Pa]
		Square	Sine	Square	Sine	Square	Sine		
Spruce	8	1.32±0.08	0.39±0.03	1.58±0.23	1.37±0.15	2.37±0.15	2.42±0.19	0.52±0.05	1.35±0.08
Fir	8	1.76±0.10	0.51±0.06	2.20±0.45	1.78±0.49	2.23±0.27	2.29±0.26	0.34±0.05	0.86±0.08
Hemlock	8	1.32±0.06	0.42±0.03	1.87±0.45	2.02±1.11	2.44±0.31	2.70±0.47	0.60±0.12	1.42±0.19
Hinoki	8	2.45±0.23	0.71±0.13	7.51±3.93	6.51±4.11	3.07±0.29	3.21±0.44	0.28±0.06	0.90±0.05
Karamatsu	6	2.07±1.03	0.64±0.31	2.33±0.83	1.81±0.58	2.57±0.64	2.62±0.29	0.43±0.30	0.99±0.45
Buna	6	1.41±0.25	0.40±0.09	2.48±0.71	2.04±0.47	2.75±0.29	2.59±0.31	0.51±0.17	1.68±0.35

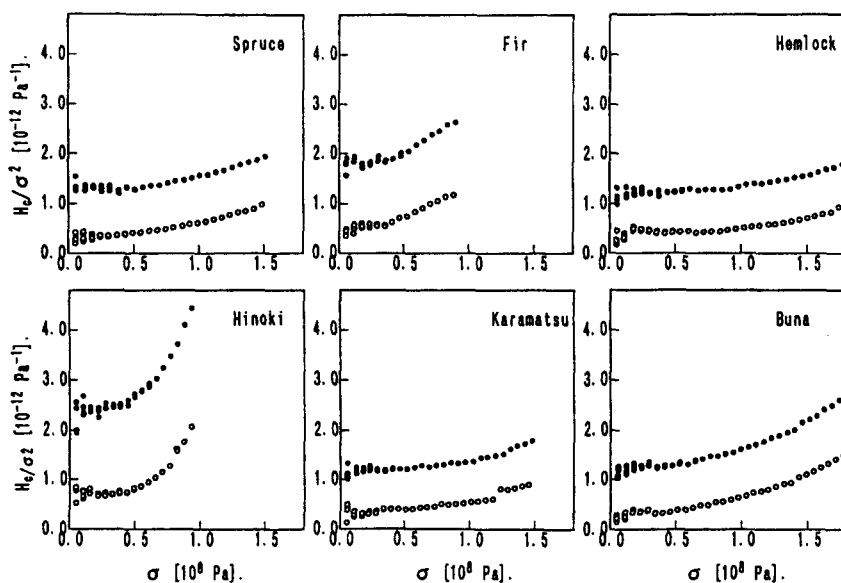


Fig. 8 Variations of energy loss behaviors among species; dependences of energy losses H_c on stress amplitude σ .

Legend: ●: Square wave, ○: Sine wave.